Constraints on the Presence of Quark Matter in Neutron Stars

J. M. Lattimer

Department of Physics & Astronomy
Stony Brook University

Collaborators: C. Drischler, K. Hebeler & A. Schwenk (Darmstadt), M. Prakash (Ohio U), A. Steiner (UT-Knoxville), Y. Lim (IBS, Daejeon, Korea)

18 March, 2015, YITP
Hadrons and Hadron Interactions in QCD 2015

Outline

- General Relativity Constraints on Neutron Star Structure
- The Neutron Star Radius and the Nuclear Symmetry Energy
- Nuclear Experimental Constraints on the Symmetry Energy
- Constraints from Pure Neutron Matter Theory
- Quark Matter in Neutron Stars
- Astrophysical Constraints on Masses and Radii

Neutron Star Structure

Tolman-Oppenheimer-Volkov equations

$$\frac{dp}{dr} = -\frac{G}{c^4}\frac{(mc^2+4\pi pr^3)(\varepsilon+p)}{r(r-2Gm/c^2)}$$

$$\frac{dm}{dr} = 4\pi\frac{\varepsilon}{c^2}r^2$$

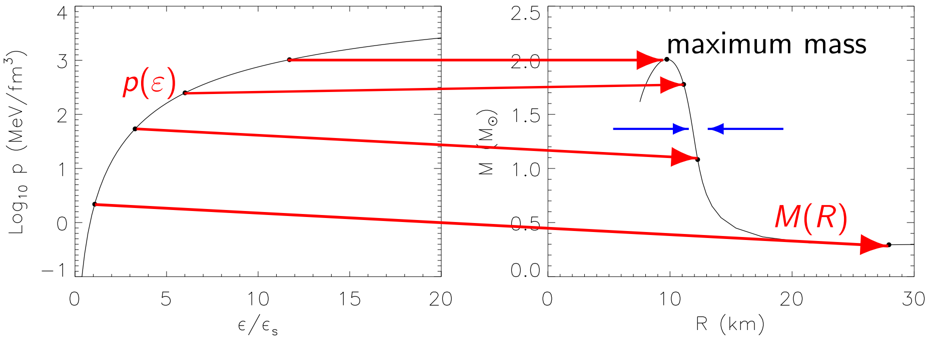

Equation of State ← Observations

Neutron Star Structure

Newtonian Gravity:

$$\frac{dp}{dr} = -\frac{Gm\rho}{r^2}; \qquad \frac{dm}{dr} = 4\pi\rho r^2; \qquad \rho c^2 = \varepsilon$$

Newtonian Polytrope:

$$p = K\rho^\gamma; \qquad M \propto K^{1/(2-\gamma)} R^{(4-3\gamma)/(2-\gamma)}$$

$$\rho < \rho_s:\ \gamma \simeq \frac{4}{3}; \qquad \rho > \rho_s:\ \gamma \simeq 2$$

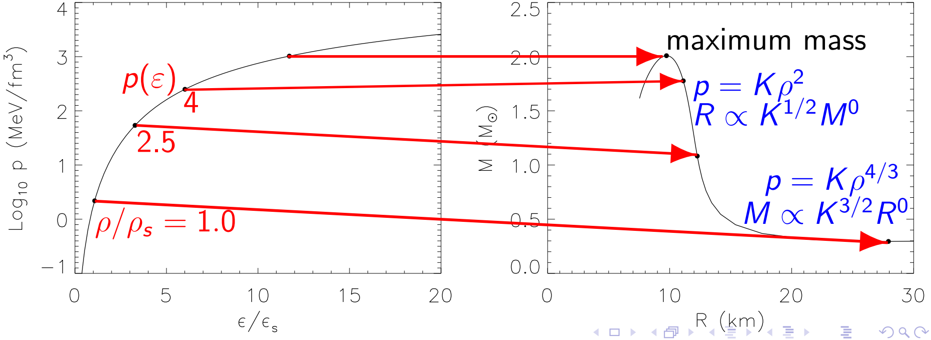

Extremes of Compaction of Neutron Stars

- The most compact and massive configurations occur when the low-density equation of state is "soft" and the high-density equation of state is "stiff" (Koranda, Stergioulas & Friedman 1997).

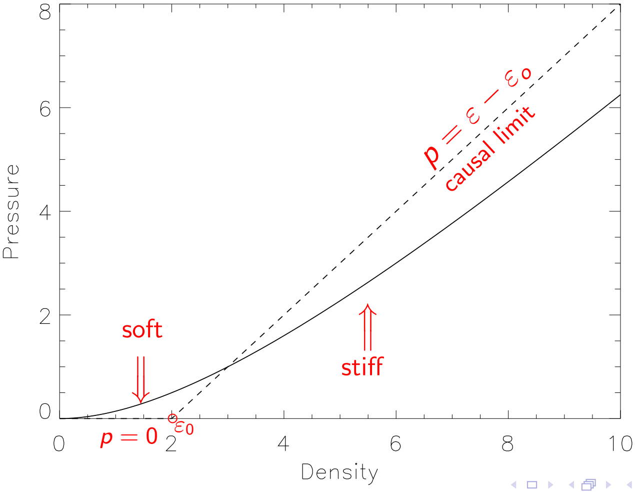

ε_0 is the only EOS parameter

The TOV solutions scale with ε_0

$w = \varepsilon/\varepsilon_0$
$y = p/\varepsilon_0$
$x = r\sqrt{G\varepsilon_0}/c^2$
$z = m\sqrt{G^3\varepsilon_0}/c^2$

Extremal Properties of Neutron Stars

The maximum mass configuration is achieved when $x_R = 0.2404$, $w_c = 3.034$, $y_c = 2.034$, $z_R = 0.08513$.

A useful reference density is the nuclear saturation density (interior density of normal nuclei):
$\rho_s = 2.7 \times 10^{14}$ g cm^{-3}, $n_s = 0.16$ baryons fm^{-3}, $\varepsilon_s = 150$ MeV fm^{-3}

- $M_{\rm max} = 4.1\ (\varepsilon_s/\varepsilon_0)^{1/2} M_\odot$ (Rhoades & Ruffini 1974)
- $M_{B,\rm max} = 5.41\ (m_B c^2/\mu_o)(\varepsilon_s/\varepsilon_0)^{1/2} M_\odot$
- $R_{\rm min} = 2.82\ GM/c^2 = 4.3\ (M/M_\odot)$ km
- $\mu_{b,\rm max} = 2.09$ GeV
- $\varepsilon_{c,\rm max} = 3.034\ \varepsilon_0 \simeq 51\ (M_\odot/M_{\rm largest})^2\ \varepsilon_s$
- $p_{c,\rm max} = 2.034\ \varepsilon_0 \simeq 34\ (M_\odot/M_{\rm largest})^2\ \varepsilon_s$
- $n_{B,\rm max} \simeq 38\ (M_\odot/M_{\rm largest})^2\ n_s$
- $\mathrm{BE}_{\rm max} = 0.34\ M$
- $P_{\rm min} = 0.74\ (M_\odot/M_{\rm sph})^{1/2}(R_{\rm sph}/10\ {\rm km})^{3/2}\ {\rm ms} = 0.20\ (M_{\rm sph,max}/M_\odot)\ {\rm ms}$

Maximum Energy Density in Neutron Stars

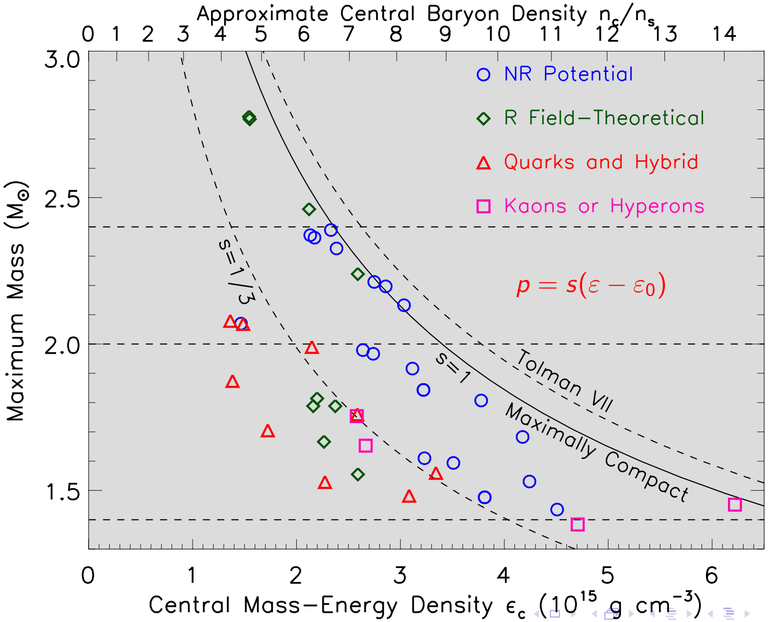

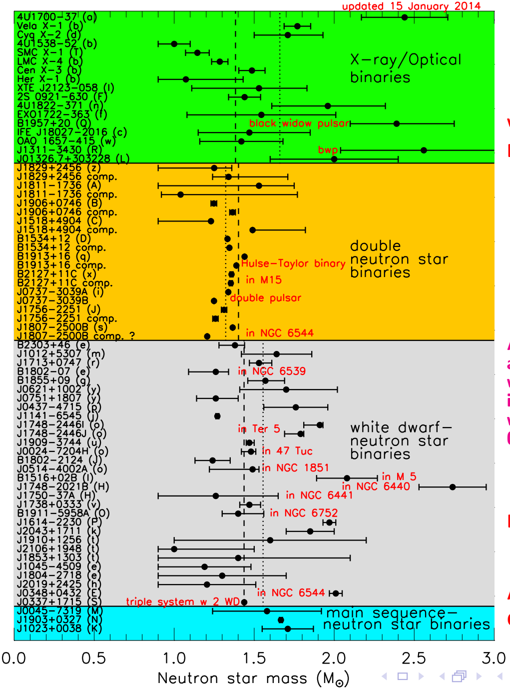

vanKerkwijk 2010

Romani et al. 2012

Although simple average mass of w.d. companions is 0.23 $M_\odot$ larger, weighted average is 0.04 $M_\odot$ smaller

Demorest et al. 2010

Antoniadis et al. 2013

Champion et al. 2008

What is the Maximum Mass?

- PSR J1614+2230 (Demorest et al. 2010)
  $M = 1.97 \pm 0.04\ M_\odot$; a nearly edge-on system with well-measured Shapiro time delay.
- PSRJ0548+0432 (Antoniadis et al. 2013)
  $M = 2.01 \pm 0.04\ M_\odot$; measured using optical data and theoretical properties of companion white dwarf.
- B1957+20 (van Kerkwijk 2010) $M = 2.4 \pm 0.3\ M_\odot$; black widow pulsar (BWP).
- PSR J1311-3430 (Romani et al. 2012)
  $M = 2.55 \pm 0.50\ M_\odot$; BWP.
- PSR J1544+4937 (Tang et al. 2014)
  $M = 2.06 \pm 0.56 M_\odot$; BWP.
- PSR 2FGL J1653.6-0159 (Romani et al. 2014)
  $M > f(M_2)/\sin^3 i \gtrsim 1.96 M_\odot$; largest $f(M_2)$.
- PSR J1227-4859 (de Martino et al. 2014)
  $M = 2.2 \pm 0.8 M_\odot$; redback pulsar.

Black Widow Pulsar PSR B1957+20

1.6ms pulsar in circular 9.17h orbit with $\sim 0.03\ M_\odot$ companion.
Pulsar is eclipsed for 50-60 minutes each orbit; eclipsing object has a volume much larger than the companion or its Roche lobe.
It is believed the pulsar is ablating the companion leading to mass loss and an eclipsing plasma cloud. Companion nearly fills its Roche lobe.
Ablation by pulsar leads to eventual disappearance of companion.
The optical light curve does not represent the center of mass of the companion, but the motion of its irradiated hot spot.

pulsar radial velocity

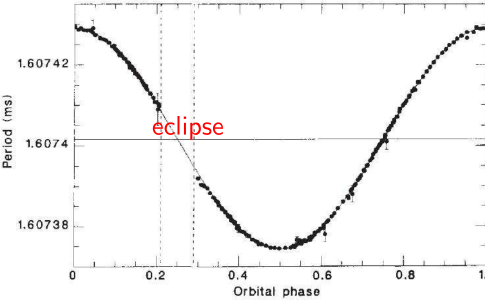

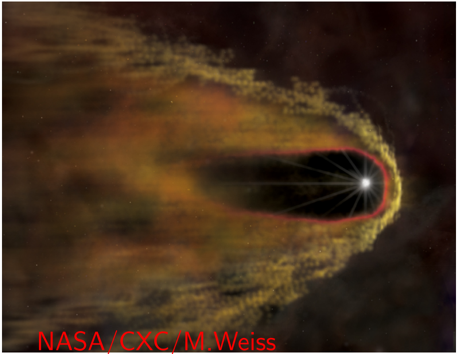

Black Widow Pulsar PSR B1957+20

$K_i = 2\pi \frac{a_i \sin i}{P}$

$q = \frac{M_P}{M_*} = \frac{a_*}{a_P} = \frac{K_*}{K_P}$

$K_* = K_{obs}\left(1 + \frac{R_*}{a_*}\right)$

Radiated area of companion has a smaller orbit than the center of mass.

$M_P = q(1+q)^2 \frac{P}{2\pi G}\left(\frac{K_P}{\sin i}\right)^3$

Modeling of light curve shape suggests that

$M_P > 1.8\ \mathrm{M}_\odot$, $\sin i < 66^\circ$

Most probable values:

$2.20 M_\odot < M_P < 2.55 M_\odot$

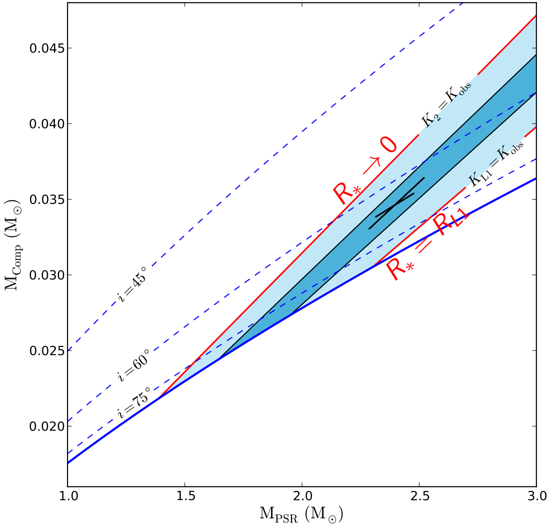

van Kerkwijk 2010

Causality + GR Limits and the Maximum Mass

A lower limit to the maximum mass sets a lower limit to the radius for a given mass.

Similarly, a precise (M, R) measurement sets an upper limit to the maximum mass.

$1.4 M_\odot$ stars must have $R > 8.15 M_\odot$.

$1.4 M_\odot$ strange quark matter stars (and likely hybrid quark/hadron stars) must have $R > 11$ km.

$M - R$ curves for maximally compact EOS

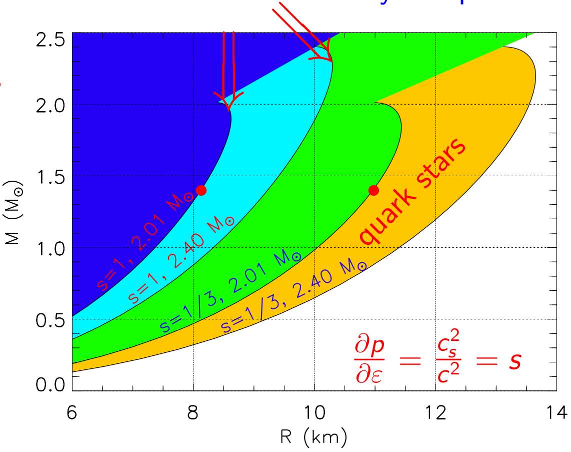

Maximum Mass and Neutron Star Radii

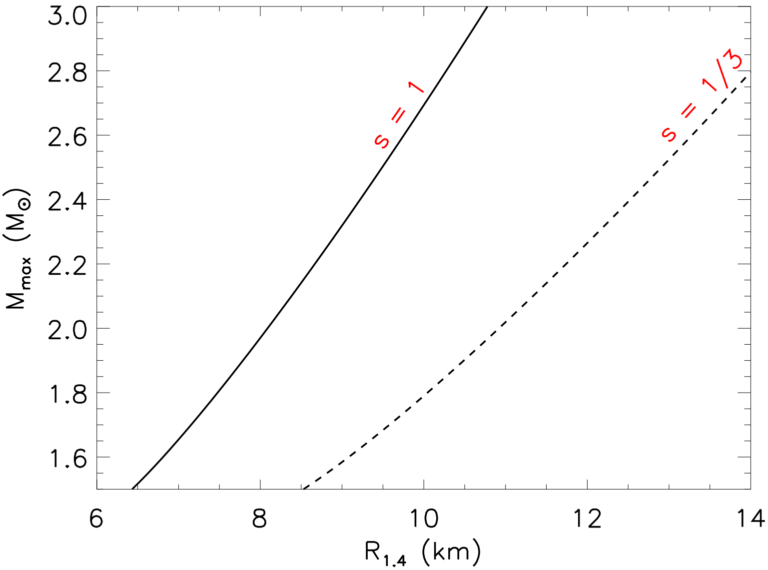

Mass-Radius Diagram and Theoretical Constraints

GR:
$R > 2GM/c^2$

$P < \infty$:
$R > (9/4)GM/c^2$

causality:
$R \gtrsim 2.9GM/c^2$

— normal NS
— SQS

— $R_\infty = \dfrac{R}{\sqrt{1-2GM/Rc^2}}$

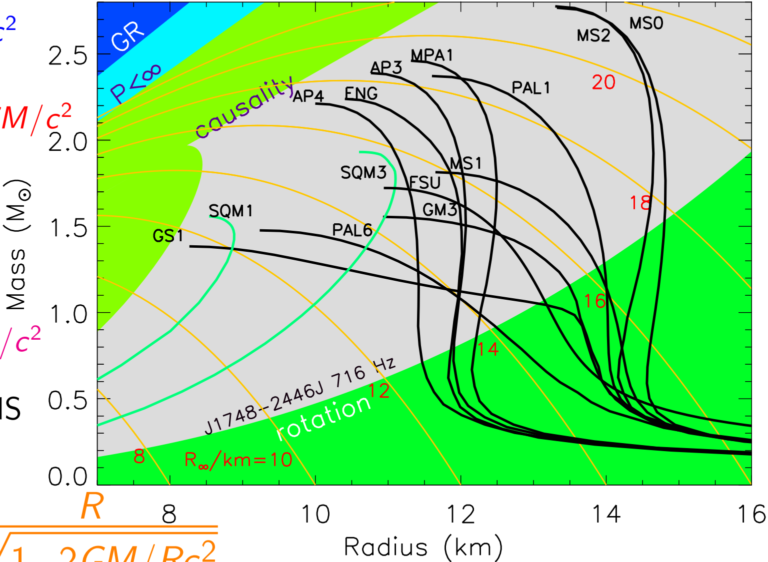

The Radius – Pressure Correlation

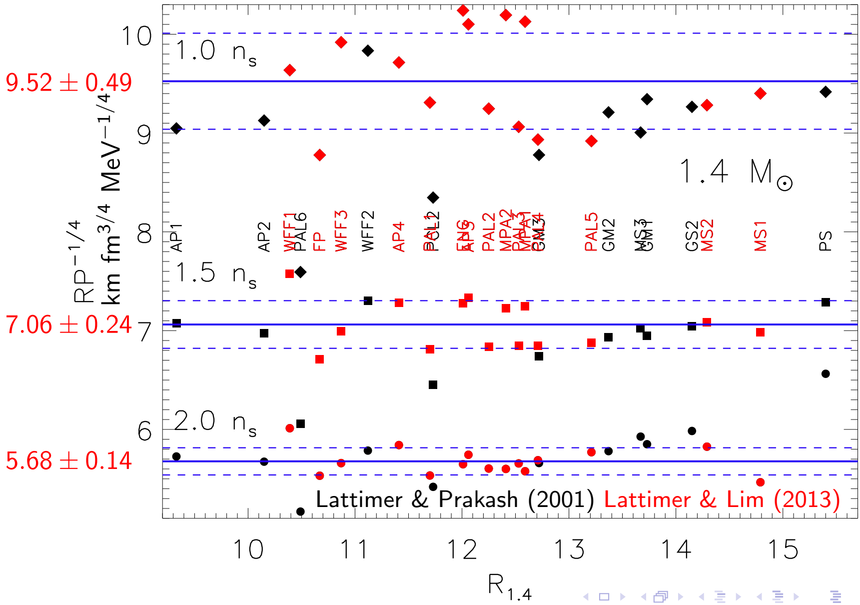

Nuclear Symmetry Energy

Defined as the difference between energies of pure neutron matter $(x = 0)$ and symmetric $(x = 1/2)$ nuclear matter.

$$S(\rho) = E(\rho, x = 0) - E(\rho, x = 1/2)$$

Expanding around the saturation density (ρ_s) and symmetric matter $(x = 1/2)$

$$E(\rho, x) = E(\rho, 1/2) + (1-2x)^2 S_2(\rho) + \ldots$$

$$S_2(\rho) = \mathbf{S_v} + \frac{\mathbf{L}}{3}\frac{\rho - \rho_s}{\rho_s} + \ldots$$

$$\mathbf{S_v} \simeq 31 \text{ MeV}, \quad \mathbf{L} \simeq 50 \text{ MeV}$$

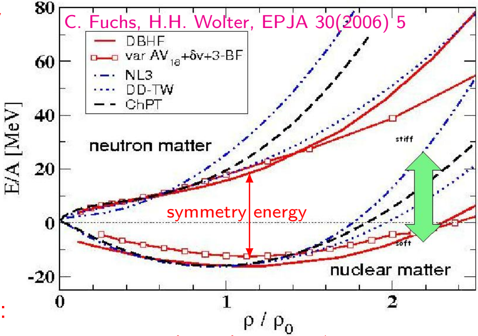

Connections to pure neutron matter:

$$E(\rho_s, 0) \approx S_v + E(\rho_s, 1/2) \equiv S_v - B, \qquad p(\rho_s, 0) = L\rho_s/3$$

Neutron star matter (in beta equilibrium):

$$\frac{\partial(E + E_e)}{\partial x} = 0, \quad p(\rho_s, x_\beta) \simeq \frac{L\rho_s}{3}\left[1 - \left(\frac{4S_v}{\hbar c}\right)^3 \frac{4 - 3S_v/L}{3\pi^2\rho_s}\right]$$

Nuclear Experimental Constraints

Binding Energies

Liquid Droplet Model

$$E_{sym} = AI^2\left[\frac{S_v}{1+S_sA^{-1/3}/S_v} - \frac{Ze^2}{20R}\frac{S_sA^{-1/3}/S_v}{1+S_sA^{-1/3}/S_v}\right]$$

$$\frac{S_s}{S_v} \simeq \frac{3a}{2r_o}\left[1+\frac{L}{3S_v}+\left(\frac{L}{3S_v}\right)^2\cdots\right]$$

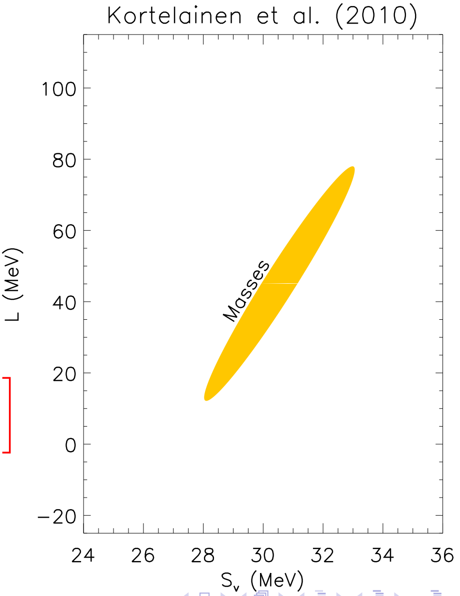

Why Symmetry Parameters are Highly Correlated

Assuming approximate validity of liquid drop model:

$$E_{\rm sym}(N,Z) = (S_v A - S_s A^{2/3}) I^2$$

$$\chi^2 = \frac{1}{\mathcal{N}\sigma_D^2} \sum_{i=1}^{\mathcal{N}} (E_{ex,i} - E_{sym,i})^2$$

$$\chi_{vv} = \frac{2}{\mathcal{N}\sigma_D^2} \sum_{i=1}^{\mathcal{N}} I_i^4 A_i^2 = 61.6\,\sigma_D^{-2}$$

$$\chi_{vs} = -\frac{2}{\mathcal{N}\sigma_D^2} \sum_{i=1}^{\mathcal{N}} I_i^4 A_i^{5/3} = -10.7\,\sigma_D^{-2}$$

$$\chi_{ss} = \frac{2}{\mathcal{N}\sigma_D^2} \sum_{i=1}^{\mathcal{N}} I_i^4 A_i^{4/3} = 1.87\,\sigma_D^{-2}$$

$$\sigma_{S_v} = \sqrt{\frac{2\chi_{ss}}{\chi_{vv}\chi_{ss}-\chi_{sv}^2}} \simeq 2.3\,\sigma_D$$

$$\sigma_{S_s} = \sqrt{\frac{2\chi_{vv}}{\chi_{vv}\chi_{ss}-\chi_{sv}^2}} \simeq 13.2\,\sigma_D$$

$$\alpha = \frac{1}{2}\tan^{-1}\frac{2\chi_{vs}}{\chi_{vv}-\chi_{ss}} \simeq 9^\circ.8$$

$$r_{vs} = -\frac{\chi_{vs}}{\sqrt{\chi_{vv}\chi_{ss}}} \simeq 0.997$$

Liquid droplet model:

$$E_{\rm sym}(N,Z) = \frac{S_v A I^2}{1+(S_s/S_v)A^{-1/3}}$$

$$S_s \simeq \frac{3a}{2r_o} S_v \left[1 + (L/3S_v) + (L/3S_v)^2\right]$$

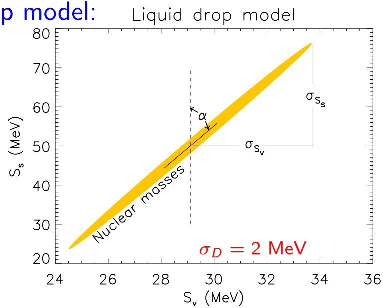

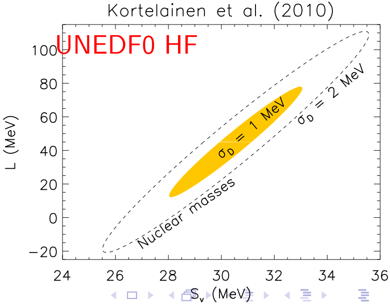

Nuclear Experimental Constraints

Neutron Skin Thicknesses

$$r_{np} = \frac{2r_o}{3S_v}\frac{1}{\sqrt{1-I^2}}\left(1 + S_s A^{-1/3}/S_v\right)^{-1}$$
$$\times\sqrt{\frac{3}{5}}\left[IS_s - \frac{3Ze^2}{140r_o}\left(1 + \frac{10}{3}\frac{S_s A^{-1/3}}{S_v}\right)\right]$$

$$r_{np,208} = 0.15 \pm 0.04 \text{ fm}$$

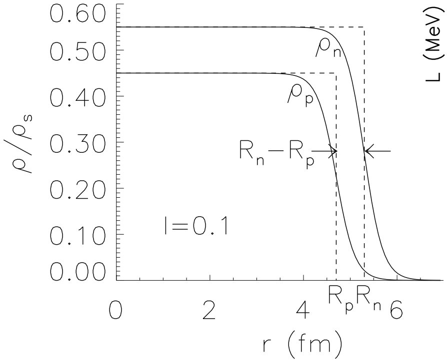

Tarbert et al. (2014)

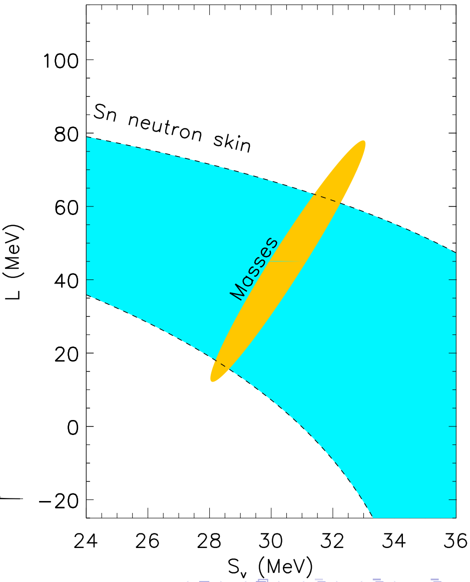

Nuclear Experimental Constraints

Flows in
Heavy Ion Collisions

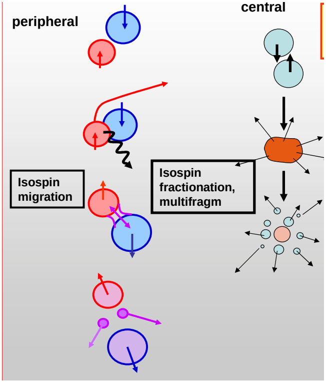

Wolter, NuSYM11

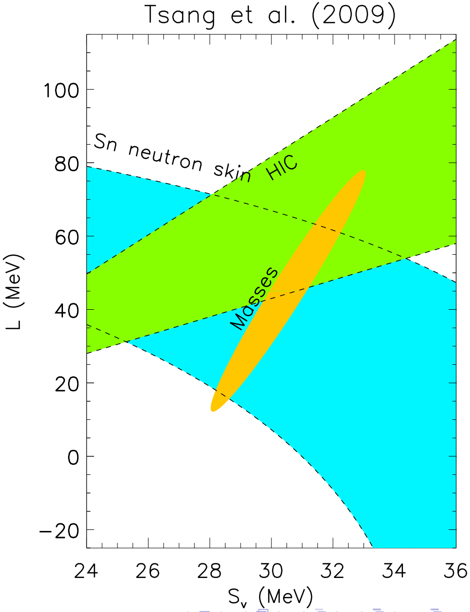

Nuclear Experimental Constraints

Giant Dipole Resonance Centroids

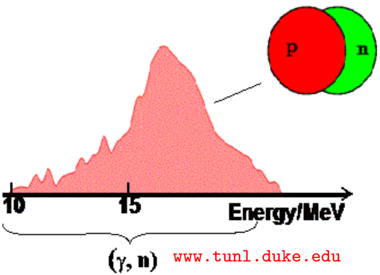

www.tunl.duke.edu

23.3 MeV$<$ $S_2(0.1\ \mathrm{fm}^{-3})$ $<$24.9 MeV

Trippa, Colo & Vigezzi (2008)

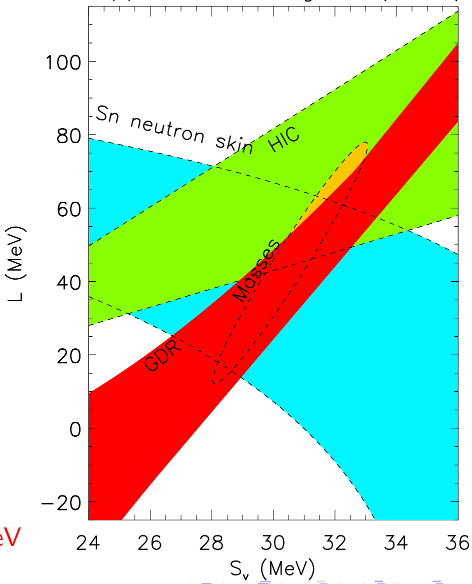

Nuclear Experimental Constraints

Dipole Polarizabilities

$\alpha_D = 4m_{-1}$

$\simeq \frac{AR^2}{20S_v}\left(1 + \frac{5}{3}\frac{S_s A^{-1/3}}{S_v}\right)$

Uses data of Tamii et al. (2011)

$\alpha_{D,208} = 20.1 \pm 0.6\ \mathrm{fm}^2$

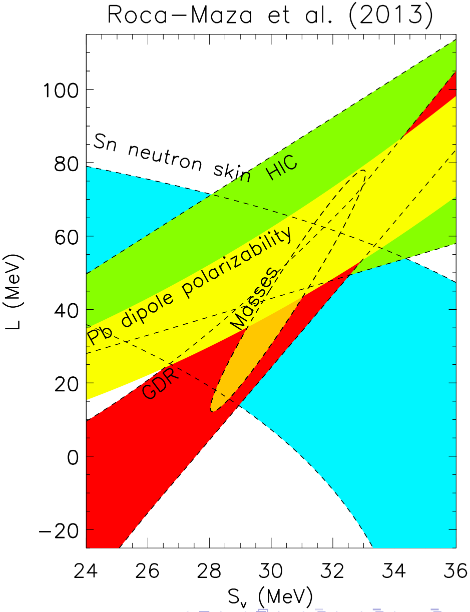

Nuclear Experimental Constraints

Isobaric Analog States

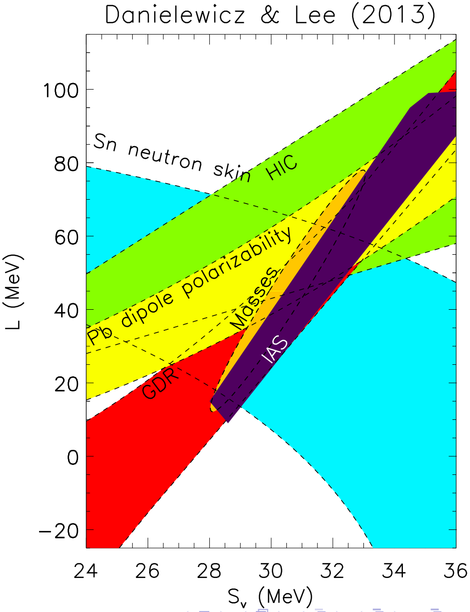

Theoretical Neutron Matter Calculations

H&S: Chiral Lagrangian

GC&R: Quantum Monte Carlo

$S_v - L$ constraints from Hebeler et al. (2012)

Gandolfi, Carlson & Reddy (2011); Hebeler & Schwenk (2011)

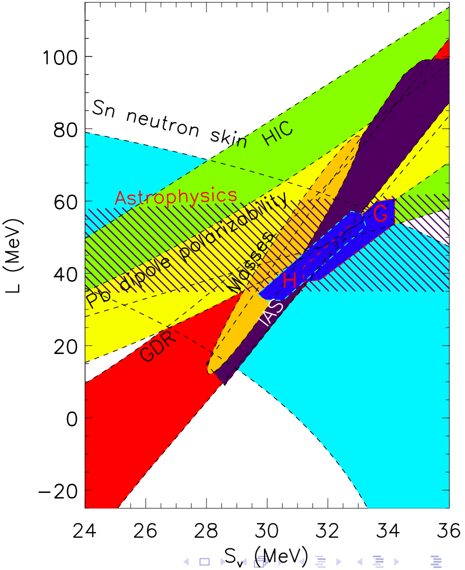

Theoretical Neutron-Rich Matter Calculations

Chiral Lagrangian studies of neutron and neutron-rich matter by Drischler, Somá & Schwenk (2014) and Drischler, Hebeler & Schwenk.

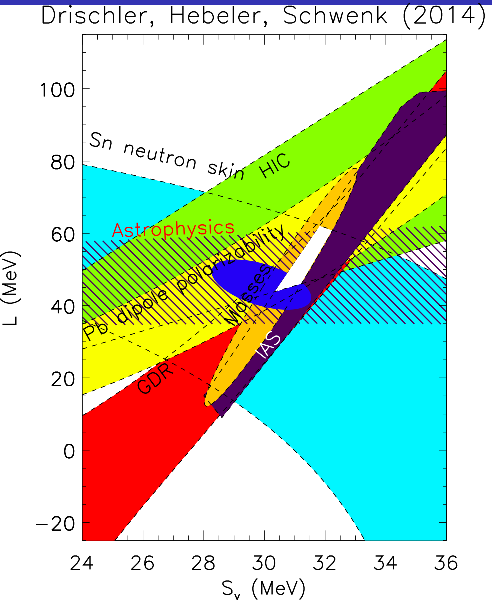

Neutron Matter Comparisons

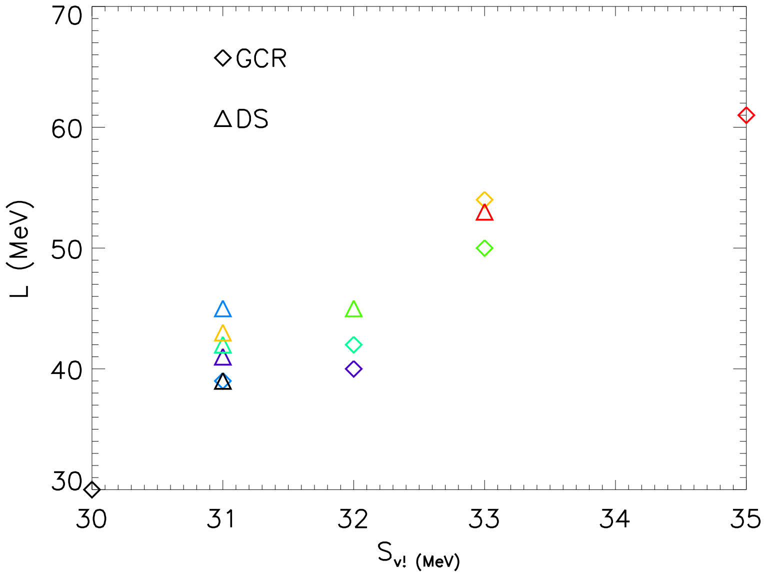

Neutron Matter Extrapolations and $M - R$

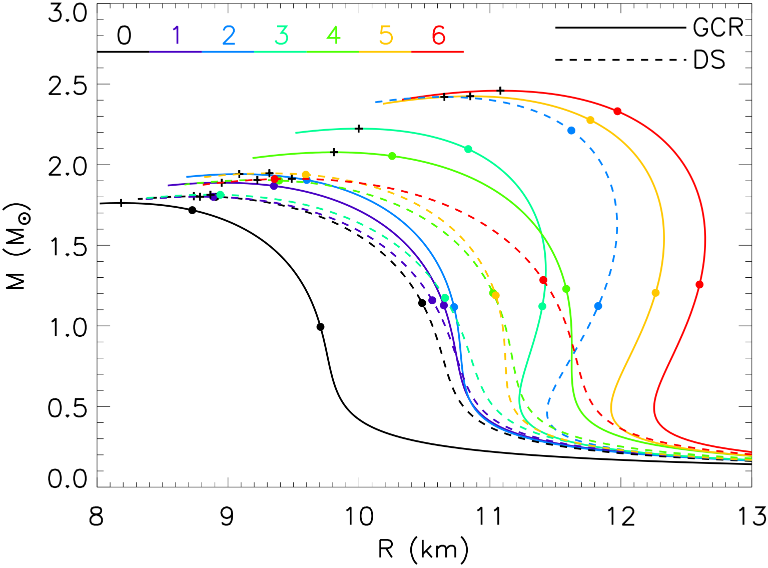

Neutron Matter Extrapolations and $M_{max} - R_{1.4}$

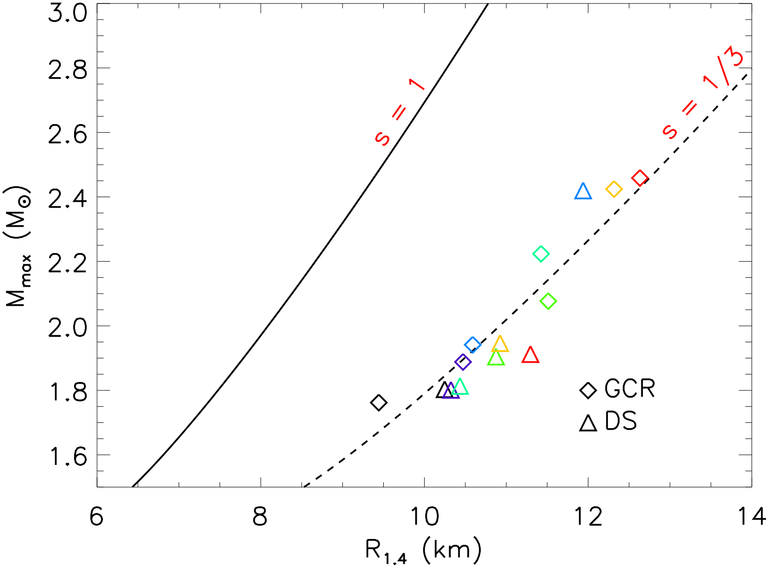

First Order Phase Transition in Neutron Stars

- Generic first order phase transiton with 3 parameters: $\Delta\varepsilon$, ε_t and P_t.
- Make 2 dimensionless parameter combinations: $\Delta\varepsilon/\varepsilon_t$ and P_t/ε_t.
- Critical condition for existence of stable hybrid core connected to normal branch (**A, D**):

$$\frac{\Delta\varepsilon}{\varepsilon_t} \leq \frac{1}{2} + \frac{3}{2}\frac{P_t}{\varepsilon_t}.$$

- It is also possible to have a stable hybrid core disconnected from normal barnch (**B, D**).
- Parametrize high-density phase with a constant sound speed $c^2_{\rm QM} = dp/d\varepsilon \sim 1/3$.

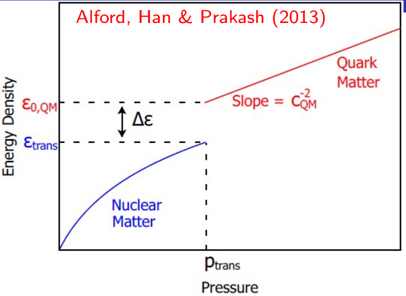

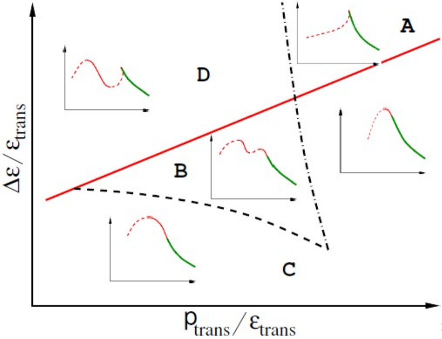

Possible Hybrid Configurations

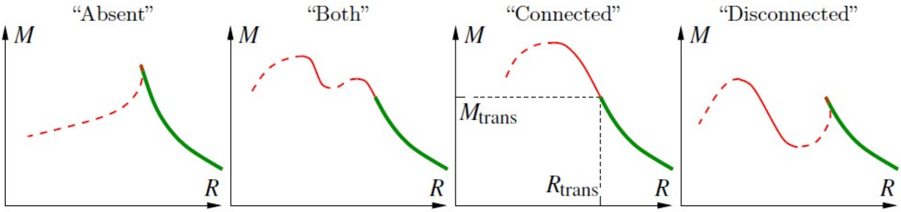

A **B** **C** **D**

Alford, Han & Prakash (2013)

Sound Speed in Quark Matter

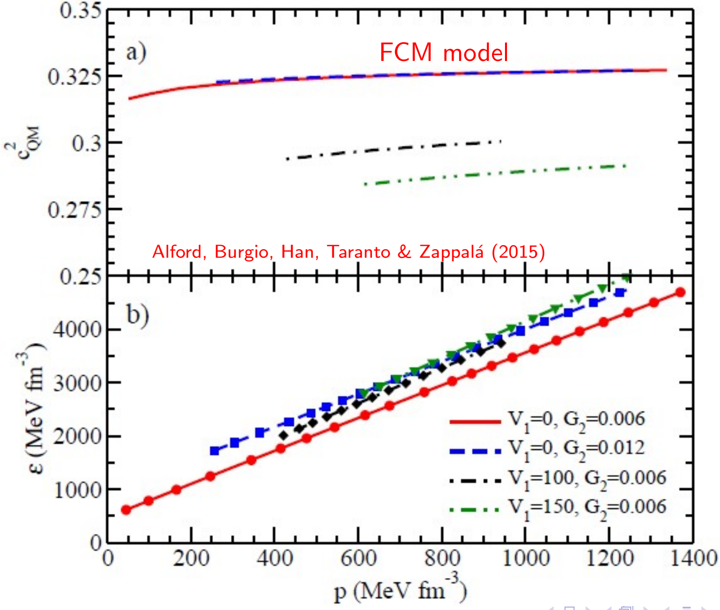

Mass Constraint

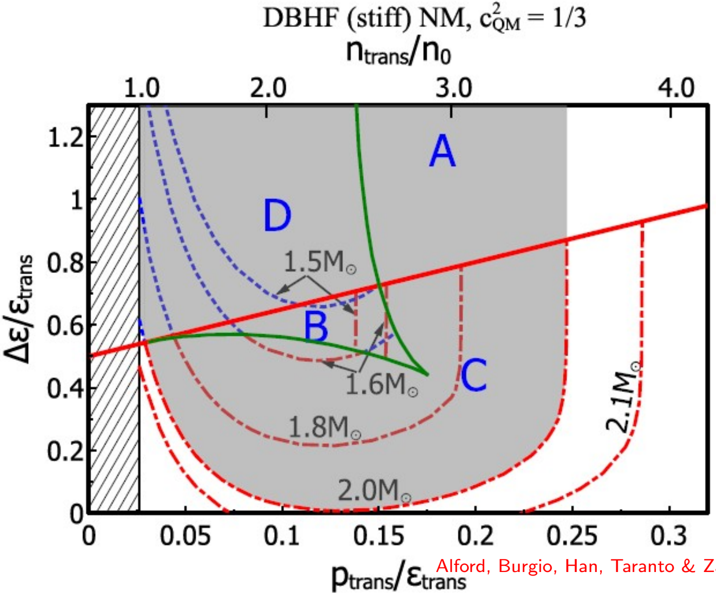

Alford, Burgio, Han, Taranto & Zappalá (2015)

Mass Constraint

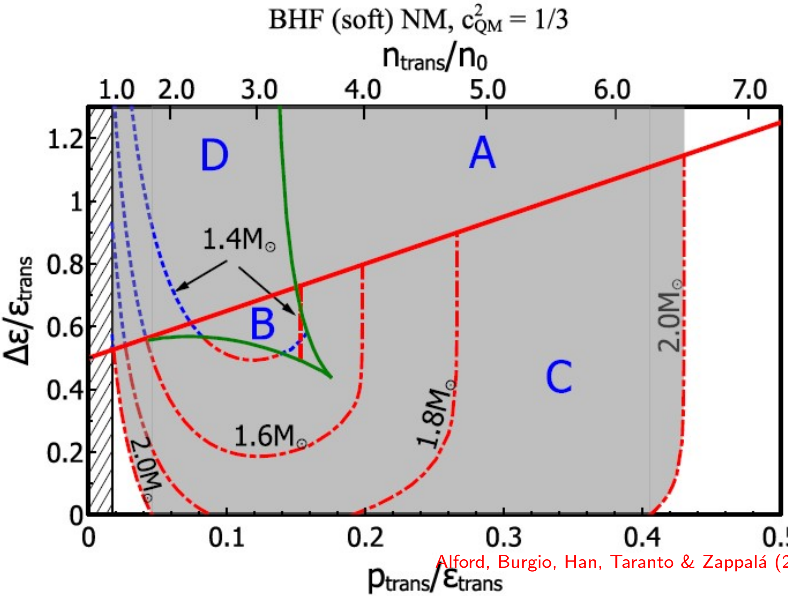

Alford, Burgio, Han, Taranto & Zappalá (2015)

Radius Constraint

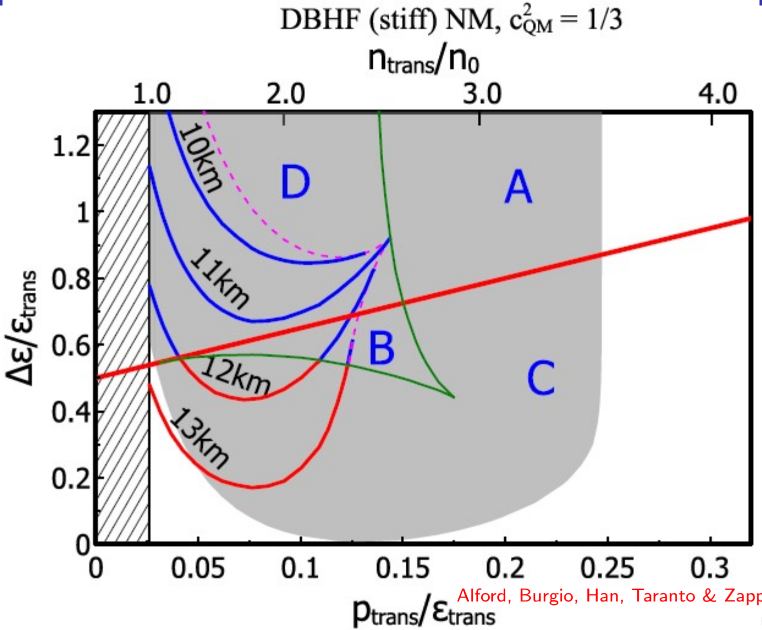

Alford, Burgio, Han, Taranto & Zappalá (2015)

Radius Constraint

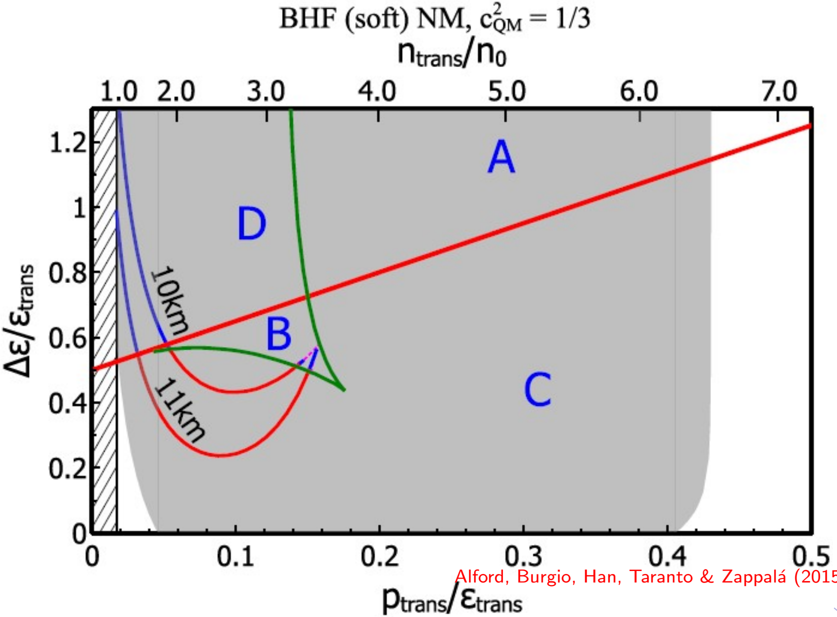

Alford, Burgio, Han, Taranto & Zappalá (2015)

Radius Constraint

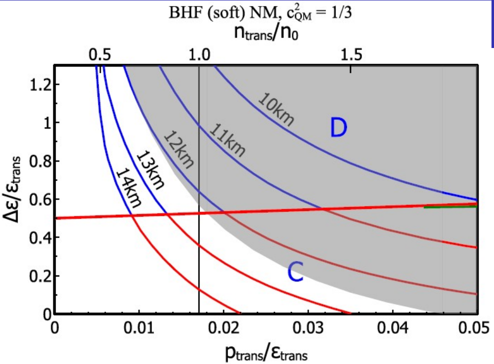

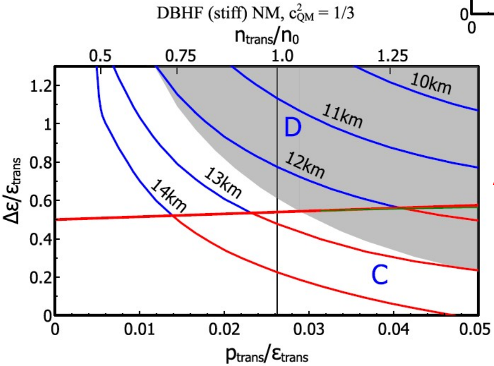

Alford, Burgio, Han, Taranto & Zappalá (2015)

$M_{max} - R_{1.4}$

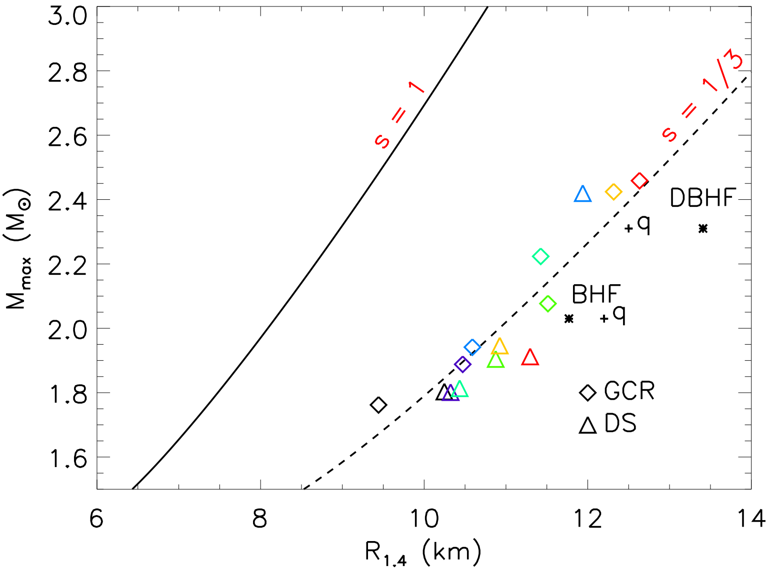

3.0
2.8
2.6
2.4
2.2
2.0
1.8
1.6
6
8
10
12
14
M_{max} $(M_\odot)$
$R_{1.4}$ (km)
s = 1
s = 1/3
DBHF
+q
BHF
+q
◇ GCR
△ DS

Simultaneous Mass/Radius Measurements

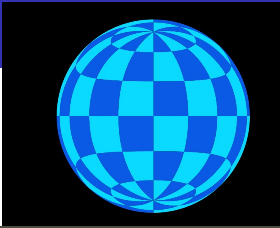

- Measurements of flux $F_\infty = (R_\infty/D)^2 \sigma T_{\rm eff}^4$ and color temperature $T_c \propto \lambda_{\rm max}^{-1}$ yield an apparent angular size (pseudo-BB):

$$\frac{R_\infty}{D} = \frac{R}{D}\frac{1}{\sqrt{1-2GM/Rc^2}}$$

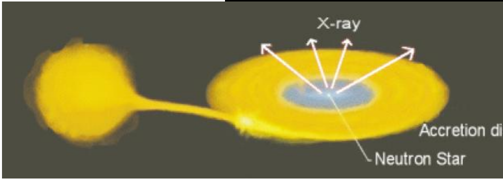

- Observational uncertainties include distance D, interstellar absorption N_H, atmospheric composition

Best chances for accurate radius measurement:

- Nearby isolated neutron stars with parallax (uncertain atmosphere)
- Quiescent low-mass X-ray binaries (QLMXBs) in globular clusters (reliable distances, low B H-atmosperes)
- Bursting sources (XRBs) with peak fluxes close to Eddington limit (where gravity balances radiation pressure)

$$F_{\rm Edd} = \frac{cGM}{\kappa D^2}\sqrt{1-2GM/Rc^2}$$

$M - R$ PRE Burst Estimates

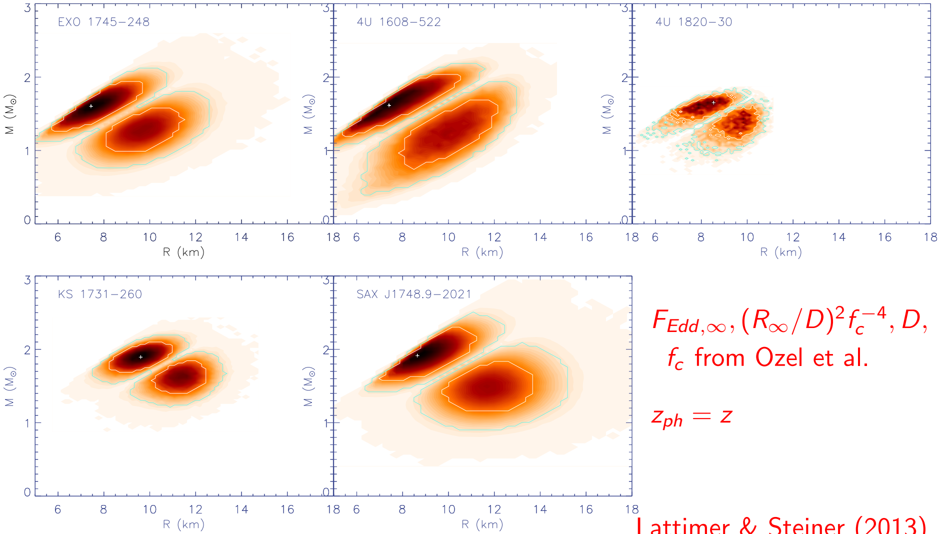

$F_{Edd,\infty}, (R_\infty/D)^2 f_c^{-4}, D,$
f_c from Ozel et al.

$z_{ph} = z$

Lattimer & Steiner (2013)

$M - R$ PRE Burst Estimates

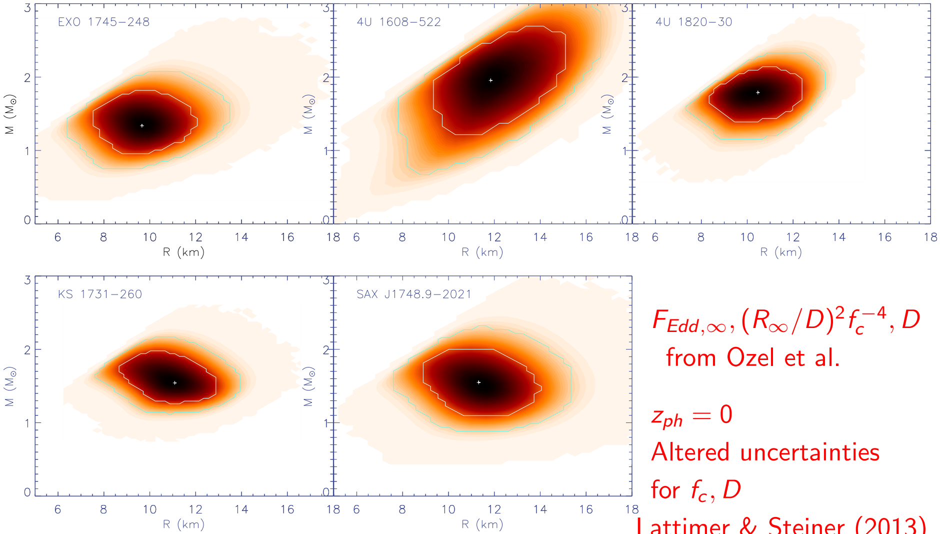

$F_{Edd,\infty}, (R_\infty/D)^2 f_c^{-4}, D$
from Ozel et al.

$z_{ph} = 0$
Altered uncertainties
for f_c, D

Lattimer & Steiner (2013)

$M - R$ QLMXB Estimates

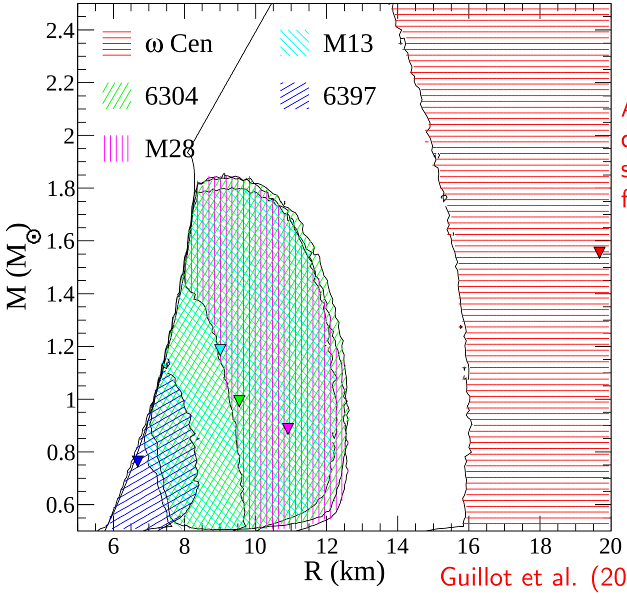

Absorption (N_H) determined self-consistently from spectra

Guillot et al. (2013)

$M - R$ QLMXB Estimates

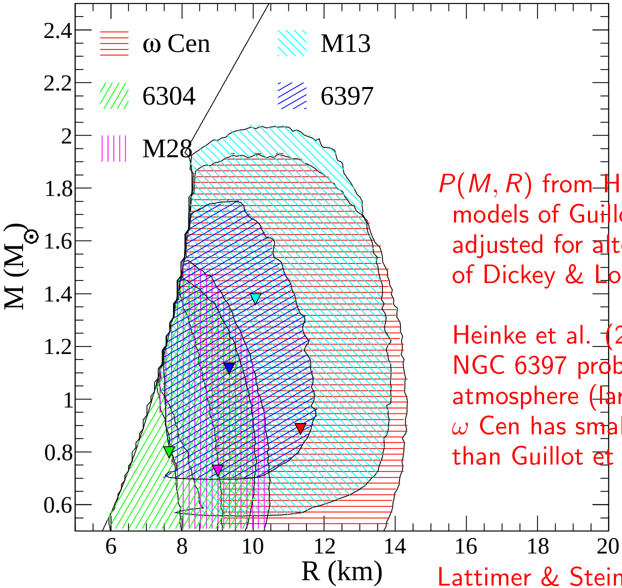

$P(M, R)$ from H atmosphere models of Guillot et al. (2013), adjusted for alternate N_H values of Dickey & Lockman (1990).

Heinke et al. (2014) found NGC 6397 probably has He atmosphere (larger R); ω Cen has smaller N_H (and R) than Guillot et al. (2013) found.

Lattimer & Steiner (2013)

Bayesian TOV Inversion

- $\varepsilon < 0.5\varepsilon_0$: Known crustal EOS
- $0.5\varepsilon_0 < \varepsilon < \varepsilon_1$: EOS parametrized by K, K', S_v, γ
- Polytropic EOS: $\varepsilon_1 < \varepsilon < \varepsilon_2$: n_1; $\varepsilon > \varepsilon_2$: n_2
- EOS parameters $K, K', S_v, \gamma, \varepsilon_1, n_1, \varepsilon_2, n_2$ uniformly distributed
- $M_{\rm max} \geq 1.97\ \mathrm{M}_\odot$, causality enforced
- All 10 stars equally weighted

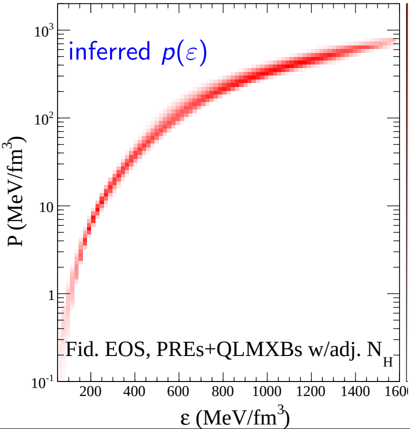

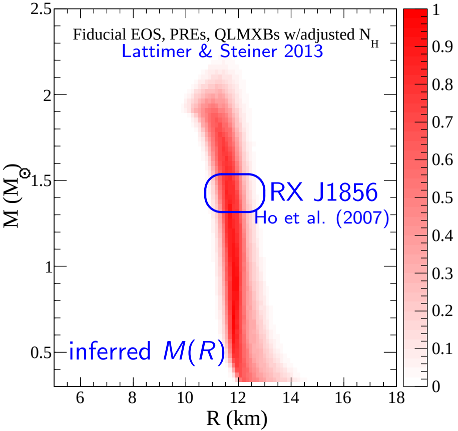

Astronomy vs. Astronomy vs. Physics

Ozel et al., PRE bursts $z_{\rm ph}$ z: $R = 9.74 \pm 0.50$ km.

Suleimanov et al., long PRE bursts: $R_{1.4} \gtrsim 13.9$ km

Guillot et al. (2013), all stars have the same radius, self N_H: $R = 9.1^{+1.3}_{-1.5}$ km.

Lattimer & Steiner (2013), TOV, crust EOS, causality, maximum mass $> 2M_\odot$, $z_{\rm ph} = z$, alt N_H.

Lattimer & Lim (2013), nuclear experiments: 29 MeV $< S_v <$ 33 MeV, 40 MeV $< L <$ 65 MeV, $R_{1.4} = 12.0 \pm 1.4$ km.

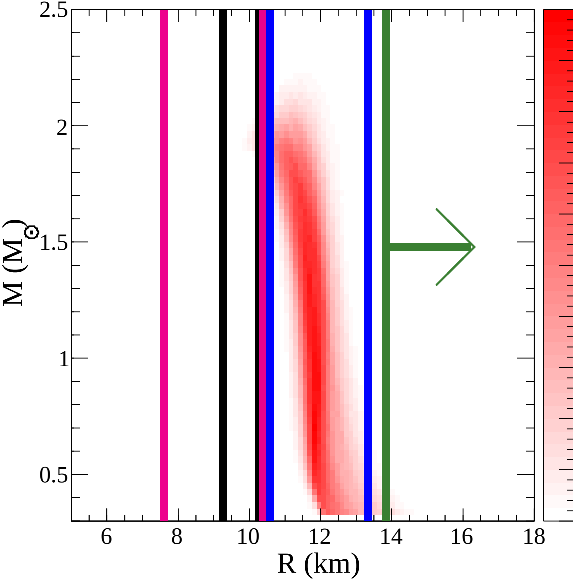

Constraints from Observations of Gravitational Radiation

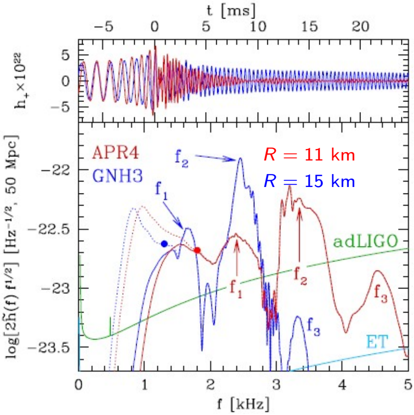

Takami, Rezzolla and Baiotti (2014)

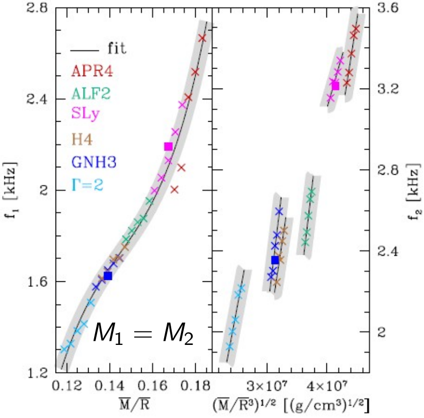

- Chirp mass and tidal deformability measurable during inspiral.
- Frequency peaks are tightly correlated with compactness.
- Mass determinations from prompt and delayed black hole formation.
- In neutron star-black hole mergers, disc mass depends on a/M_{BH} and on $M_{NS}M_{BH}/R^2$.
- R-mode instabilities in rotating neutron stars.

Additional Proposed Radius and Mass Constraints

- Pulse profiles
  Hot or cold regions on rotating neutron stars alter pulse shapes: NICER and LOFT will enable timing and spectroscopy of thermal and non-thermal emissions. Light curve modeling → M/R; phase-resolved spectroscopy → R.
- Moment of inertia
  Spin-orbit coupling of ultra-relativistic binary pulsars (e.g., PSR 0737+3039) vary i and contribute to $\dot{\omega}$: $I \propto MR^2$.
- Supernova neutrinos
  Millions of neutrinos detected from a Galactic supernova will measure BE$= m_B N - M$, $< E_\nu >$, τ_ν.
- QPOs from accreting sources
  ISCO and crustal oscillations

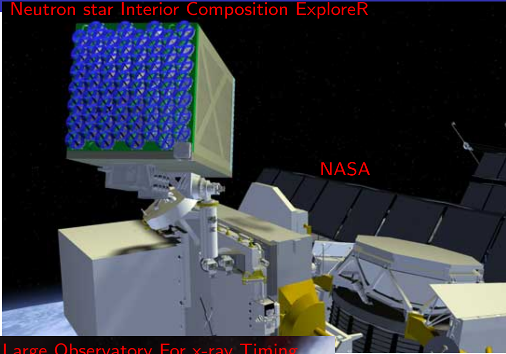

Neutron Matter Extrapolations and $M_{max} - R_{1.4}$

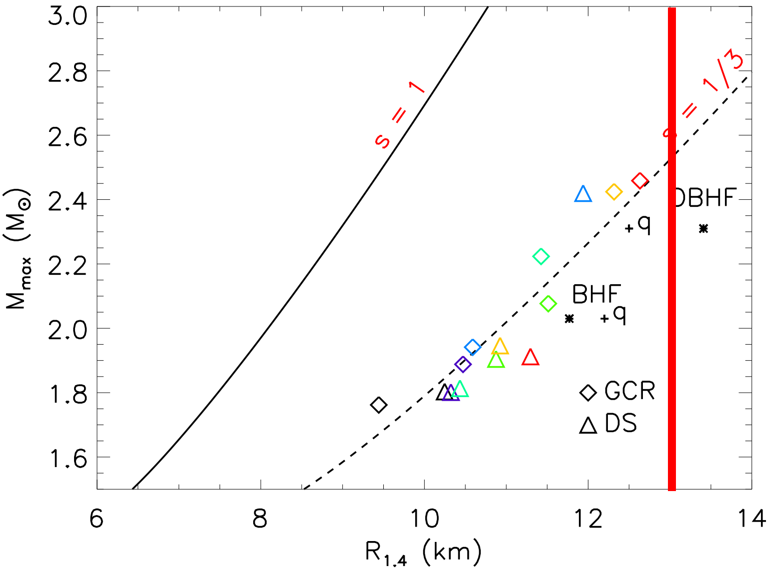

Conclusions

- Measured neutron star masses imply lower limits to radii of typical neutron stars.
- Symmetry energy determines typical neutron star radii.
- Nuclear experiments set reasonably tight constraints on symmetry energy parameters.
- Theoretical calculations of pure neutron matter predict very similar symmetry constraints.
- These constraints predict neutron star radii $R_{1.4}$ in the range 12.0 ± 1.4 km.
- Combined astronomical observations of photospheric radius expansion X-ray bursts and quiescent sources in globular clusters suggest $R_{1.4} \sim 12.1 \pm 0.6$ km.
- The properties of a high-density phase, such as quark matter, are tightly constrained by current mass measurements.
- A mass measurement above $2.4 M_{\odot}$ may be incompatible with other constraints, assuming GR is correct.

Consistency with Neutron Matter and Heavy-Ion Collisions